Laser-induced fluorescence measurements of argon ion velocities near the sheath boundary

of an argon–xenon plasma

Laser-induced fluorescence measurements of argon ion velocities near the sheath boundary of an argon–xenon plasma

Dongsoo Lee[1]**, Greg Severn**[2]**, Lutfi Oksuz**[1,3]** and Noah Hershkowitz**[1]

[1] Department of Engineering Physics, University of Wisconsin, Madison, WI 53706, USA
[2] Department of Physics, University of San Diego, San Diego, CA 92110, USA
[3] Department of Physics, Suleyman Demirel University, Isparta, Turkey

E-mail: hershkowitz@engr.wisc.edu

Abstract

The Bohm sheath criterion in single- and two-ion species plasma is studied with laser-induced fluorescence using a diode laser. Xenon is added to a low pressure unmagnetized dc hot filament argon discharge confined by surface multidipole magnetic fields. The Ar II transition at 668.614 nm is adopted for optical pumping to detect the fluorescence from the plasma and to measure the argon ion velocity distribution functions with respect to positions relative to a negatively biased boundary plate. The structures of the plasma sheath and presheath are measured by an emissive probe. The ion concentrations of the two-species in the bulk plasma are calculated from ion acoustic wave experiments. Results are compared with previous experiments of Ar–He plasmas in which the argon ions were the heavier ion species. Unlike the previous results, the argon speed is slower than its own Bohm velocity near the sheath–presheath boundary in the Ar–Xe plasma where argon ions are the lighter ion species. We argue that this result is consistent with the behaviour of the helium ion required by the generalized Bohm criterion in the previous experiments with Ar–He plasmas. Further, our results suggest that the measured argon ion speed approaches the ion sound speed of the system.

(Some figures in this article are in colour only in the electronic version)

1. Introduction

Understanding how ions gain their energy and how ion fluxes are determined at plasma boundaries remains a critical problem of plasma science. Nearly all practical plasma systems from ultra large scale integration (ULSI) processing plasmas for micro-electronic and photonic materials to plasmas for fusion research depend on multiple-ion species. Sensitive experimental tests of plasma boundary theory in such plasma systems are necessary to provide the scientific underpinning for advances in simulations as well as theory. They are necessary even to corroborate the physics of Langmuir probes. In plasmas containing multiple-ion species, what physical properties determine the flux of ions reaching the sheath edge? How is the self-consistent problem of plasma space potential formation and ion flow solved in the plasma when there are different ion species present, each with differing collisionalities? In weakly collisional plasmas with single-ion species, when the ion collisional mean free path is significantly larger than the Debye length, the Bohm criterion [1] furnishes an answer; a presheath [2, 3] sets up in the plasma so as to accelerate the ions to the Bohm velocity C_s at the sheath edge which is the ion sound speed in the bulk plasma,

$$C_s = \sqrt{T_e/m_i}, \tag{1}$$

where T_e is the electron temperature measured in eV and m_i is the ion mass.
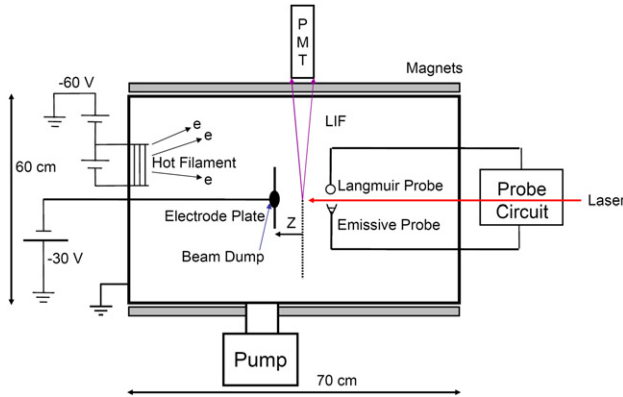
Figure 1. Schematic of the dc multidipole chamber and measurement systems.

Figure 2. Schematic diagram of the LIF experiment: (1) laser head, (2) iris, (3) iodine cell, (4) mechanical chopper, (5) periscope, (6) mirrors, (7) chamber, (8) electrode plate and beam dump, (9) photomultiplier tube, (10) wavemeter, (11) chopper controller, (12) laser driver, (13) PC, (14) oscilloscope and (15) lock-in amplifier. The arrows indicate the direction of the signal flow.

Until recently, many authors quite naturally assumed that for multiple-ion species plasmas, each ion species reaches the sheath edge with a speed equal to its own Bohm velocity [4–6]. However, theorists have recently pointed out that the generalized Bohm criterion is not a good prescription of the speeds that individual ion species have at the sheath edge [7–10], and that it is possible for ion species to reach the sheath edge with speeds which differ considerably from the single-species Bohm velocity. The first experimental hints of this came from Hala's preliminary ion acoustic wave (IAW) measurements suggesting that in Ar–He plasmas, argon ions reach the sheath edge with the velocity close to the ion sound speed of the bulk plasma, which is intermediate between the two individual ion sound speeds, the argon ions being the slow ions and the helium ion being the fast ions [11]. That the argon ions reach the sheath edge travelling much faster than its Bohm velocity was later directly corroborated with laser-induced fluorescence (LIF) measurements using diode lasers [12, 13]. However, the helium ion velocity distribution functions (ivdfs) could not be directly examined using LIF techniques. More recent IAW measurements [14], benchmarked by the LIF measurements in the vicinity of the sheath of Ar–He plasmas, have borne out this finding, leading to the urgency to determine the ivdfs of both the fast and slow ions in the two-ion species plasmas. So the question remains: what is really happening with the other ion species?

The experiments reported here directly address the issue of what happens to the argon ions when they play the role of the fast ion in a two-ion species plasma. In what follows, our experiment in a weakly collisional argon–xenon plasma is described. The LIF and electrostatic probe diagnostics are described in section 2. The results of our experiments are set out in section 3 and our summary is given in section 4. We have found that in Ar–Xe plasmas, argon ions reach the sheath edge travelling much slower than the single-ion Bohm velocity, and indeed, their speed is very close to the ion sound speed of the bulk plasma.

2. Experimental Setup

2.1. DC multidipole plasma chamber

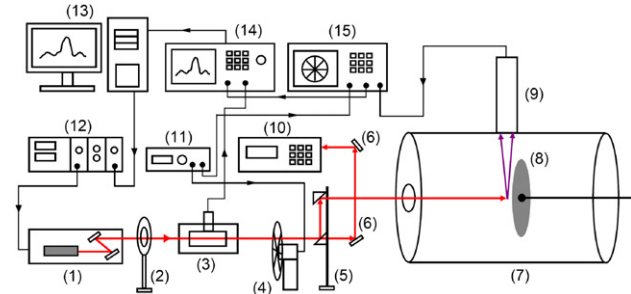A schematic diagram of the experimental arrangement employed for this study is shown in figure 1. The experiments

were carried out in a multidipole dc plasma chamber which is described in greater detail elsewhere [15]. The plasma was generated in a stainless steel chamber with an inner diameter of 60 cm and a length of 70 cm. Argon and xenon were ionized by energetic electrons emitted from hot thoriated tungsten filaments biased at -60 V with respect to the chamber wall. The cylindrical surface of the chamber was surrounded by a multidipole array of permanent magnets to improve the plasma density and uniformity. The system had a base pressure of 1×10^{-6} Torr using a turbomolecular pump backed by a rotary pump, and the operating pressure was varied from 0.5 to 0.8 mTorr depending on the experimental conditions. A stainless steel plate 15 cm in diameter biased at -30 V was placed along the axial direction in the chamber. The centre of the plate had a 1 cm diameter hole, and a razor blade stack was placed behind the hole as a beam dump. The plate was displaced with respect to the optical axis of the light collection assembly in order to measure the argon ion velocity as a function of distance from the electrode plate (z).

2.2. Argon LIF scheme and apparatus

A three-level Ar II scheme, first proposed by Severn *et al* [16], was employed in our study. In this approach, the laser with a wavelength of 668.614 nm (in vacuum) excites the $3d^4F_{7/2}$ argon ion metastables to the $4p^4D_{5/2}$ level. Radiation from the $4p^4D_{5/2}$ to $4s^4P_{3/2}$ fluorescence with a wavelength of 442.72 nm (in air) was measured. It was assumed that the argon metastable ions were in thermal equilibrium with ground state argon ions [17].

Figure 2 shows a schematic drawing of the LIF system used in this experiment. The tuneable diode laser was a Sacher Lasertechnik model Lynx-TEC 100 (SAL-665-25) with a Littrow cavity geometry, which was controlled by a modular laser driver MLD 1000. The laser had an operated power of 23 mW at a current of 85 mA and a wavelength of 668.6 nm. Fine tuning was carried out by changing the voltage on the piezoelectric actuator (V_{PZT}) with a PC. The maximum mode-hop-free tuning range was about 9 GHz, which was enough to measure the ivdfs of our plasma. The laser power variations were less than 1.5 % within our tuning range.

The laser passed through an iodine cell to acquire the iodine fluorescence spectrum simultaneously with the Ar II
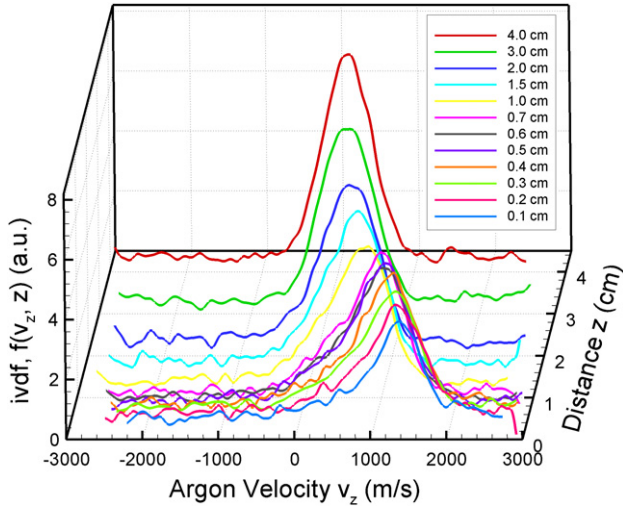
Figure 3. A family of ivdfs for the Ar–Xe plasma as a function of the distance z from the electrode plate.
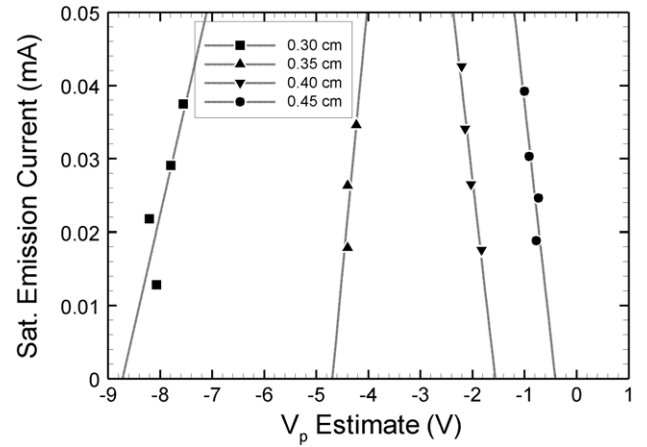

Figure 4. Determination of the sheath–presheath boundary with the emissive probe. The boundary is identified as the location where the sign of the slope changes. The sheath boundary is between 0.35 and 0.40 cm in this figure.

fluorescence. The iodine spectrum was used for a wavelength calibration [18, 19]. An iris was placed close to the laser head to block the retro-reflections from the iodine cell. The iodine cell was enclosed in an aluminium housing and heated to increase the iodine vapour pressure. The iodine fluorescence was detected by an Optek OPSL805 phototransistor. The laser beam was directed either to a Burleigh WA-1000 wavemeter or to the chamber by a rotatable periscope. The wavemeter was used to find a rough tuning range at first, and the entire beam was injected into the chamber after tuning. The Ar II fluorescence radiation was collected at $90°$ with respect to the laser beam and the electrode plate axis. It was filtered by a 0.3 nm bandwidth interference filter centred at 442.6 nm after passing an optical collection assembly which consisted of two plano-convex lenses (focal length = 8.0 and 5.0 cm) and a pinhole. Then the fluorescence was amplified by a Hamamatsu R6094 photomultiplier tube. A Stanford Research SR540 mechanical chopper spun at 3.1 kHz and an SR850 DSP lock-in amplifier were used to recover the LIF signal from the ambient background noise. The recovered LIF signal was averaged over 5 scans then smoothed. All data were controlled and collected by a data processing programme using a PC.

2.3. Ion velocity distribution function

The LIF signal collected as a function of the laser frequency (ν) was converted to an ivdf $f(v_z, z)$ using the first order Doppler shift,

$$v_z = \frac{c\Delta\nu}{\nu_0 + \Delta\nu} \approx \frac{c\Delta\nu}{\nu_0} = \lambda_0\Delta\nu, \tag{2}$$

where v_z is the ion velocity, c is the speed of light, λ_0 is the resonance wavelength (668.614 nm), ν_0 is the resonance frequency (c/λ_0) and $\Delta\nu$ is the frequency shift ($\nu-\nu_0$). Since the line width of the laser ($\approx$10 MHz) is much smaller than the expected Doppler shift for room temperature argon ions ($\approx$1 GHz), the LIF signal is proportional to the ivdf along the beam direction z, as opposed to a velocity space convolution of the ivdf. Figure 3 shows the ivdfs at different z positions relative to the negatively biased electrode plate in the Ar–Xe plasma. The neutral argon pressure is 0.5 mTorr and 0.1 mTorr

of xenon is added. At $z = 4.0$ cm from the plate, the ivdf is nearly symmetric and slightly shifted to faster velocity. The asymmetric ivdfs close to the electrode plate indicate the presence of faster ions accelerated to the plate. The one-dimensional fluid velocities were calculated from the second moment of the ivdfs,

$$\langle v_z^2 \rangle = \frac{\int_{-\infty}^{\infty} v_z^2 f(v_z, z)\,\mathrm{d}v_z}{\int_{-\infty}^{\infty} f(v_z, z)\,\mathrm{d}v_z}, \tag{3}$$

which yields the root mean square velocity $v_{\mathrm{rms}} = \langle v_z^2 \rangle^{1/2}$. In the calculations using experimental data, both the integrals in (3) were performed over a finite domain. At each z location, the baseline for the ivdf was obtained by fitting a Maxwellian velocity distribution to the data. The domain was then chosen as the region between the first negative-valued data points on each side of the main ivdf peak after a base line was subtracted from the data. The domain was the same for both the integrals of the numerator and denominator in (3).

2.4. Emissive and Langmuir probe

An emissive probe was used to measure the plasma potential (V_p) as a function of the distance z using the inflection point method in the limit of zero emission [20]. The filament was made of a tungsten wire 0.025 mm in diameter and approximately 3 mm long. The emissive probe was moved along the central axis of the electrode plate. The inflection points were identified by differentiating the I–V curves of the emissive probe. The sheath–presheath boundary was determined as the position where the voltages of the inflection points changed from increasing with emission to decreasing with emission [21]. Figure 4 shows an example of the voltage variations of the inflection points with the saturated electron emission current in the 0.7 mTorr argon plasma. It is evident that the voltages of the inflection points increase with emission at 0.30 and 0.35 cm and decrease with emission at 0.40 and 0.45 cm. This indicates that the sheath–presheath boundary is between 0.35 and 0.40 cm.

A Langmuir probe was employed to measure the electron density and temperature in the bulk plasma far from the
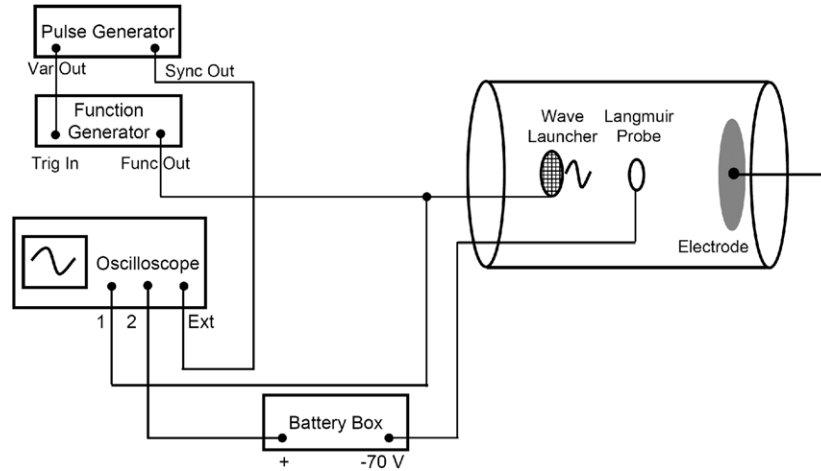
Figure 5. Schematic of the ion acoustic wave measurement system. A sinusoidal tone burst is launched from the grid and ion saturation current is collected by the Langmuir probe.

electrode plate ($z = 15$ cm) and chamber wall. The probe tip was constructed of a tungsten disc 0.95 cm in diameter. The Langmuir probe data showed that two Maxwellian electron components existed in our plasmas. The effective electron temperature (T_e) used for the calculation of the Bohm velocity was calculated as a harmonic average of the two temperatures with density weighting [22],

$$\frac{1}{T_e} = \left(\frac{n_c}{n_e}\right)\frac{1}{T_c} + \left(\frac{n_h}{n_e}\right)\frac{1}{T_h}, \tag{4}$$

where n_e is the total electron density, n_c and n_h are the cold and hot electron densities and T_c and T_h are the cold and hot electron temperatures, respectively.

2.5. IAW measurement

Ion acoustic waves (IAWs) are the oscillation of ions in the direction of the applied or perturbed electric field and they move with the ion sound speed of the system. The ion acoustic waves were generated by means of a grid immersed in the plasma. A schematic diagram of the IAW experiments is shown in figure 5. The grid was made of a stainless steel mesh 2.5 cm in diameter, which was located at a fixed position on the central axis. The electrode plate was pulled back near the wall to avoid possible interference. A tone burst consisting of two periods of a sinusoidal wave with peak-to-peak amplitude of 5 V was given to the grid in order to launch the ion waves. The pulse frequency was 200 kHz which was lower than the ion plasma frequencies of which values were approximately 2 MHz in our plasmas. For low amplitude, low frequency ion acoustic waves, the group velocity v_g equals the phase velocity v_{ph}. A negatively biased Langmuir probe was moved from the grid and the delay in the arrival time was detected. The ion sound speed of the system which was equal to the phase velocity in the bulk plasma was determined from the slope of the phase delays versus the receiving probe positions. Then each ion concentration in the bulk plasma was calculated from the measured IAW phase velocities (v_{ph}) in the Ar–Xe plasmas expressed as [23]

$$v_{ph} = \sqrt{(n_{Ar}/n_e)C_{Ar}^2 + (n_{Xe}/n_e)C_{Xe}^2}. \tag{5}$$
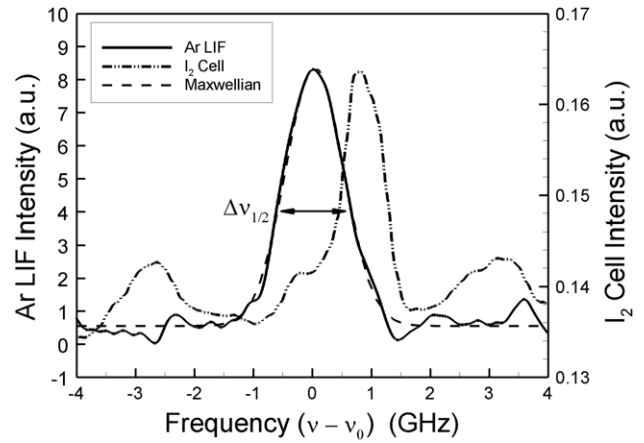

Figure 6. Measured argon ivdf in the bulk region of the pure argon plasma and the iodine cell spectrum. The Ar LIF is fitted to a Maxwellian distribution to calculate the FWHM frequency $\Delta\nu_{1/2}$. The iodine cell spectrum is used for the frequency calibration.

Given charge neutrality, the ratios of each ion concentration to the electron density were calculated with the electron temperature (T_e) measured by the Langmuir probe.

3. Experimental results and discussion

3.1. Argon ion velocities in pure argon plasma

The LIF signal measured in the bulk region of the pure argon plasma is given in figure 6. The neutral pressure of argon is 0.7 mTorr. The electrode plate is grounded and pulled back toward the side wall of the chamber. The observed distribution function appears nearly Maxwellian. For the Maxwellian distribution function, the ion temperature is given by

$$T_i = \frac{m_i c^2}{8\ln 2}\left(\frac{\Delta\nu_{1/2}}{\nu_0}\right)^2, \tag{6}$$

where T_i is the ion temperature, m_i is the ion mass, $\Delta\nu_{1/2}$ is the Doppler-broadened full width at half maximum (FWHM) frequency and ν_0 is the central (resonance) frequency. For
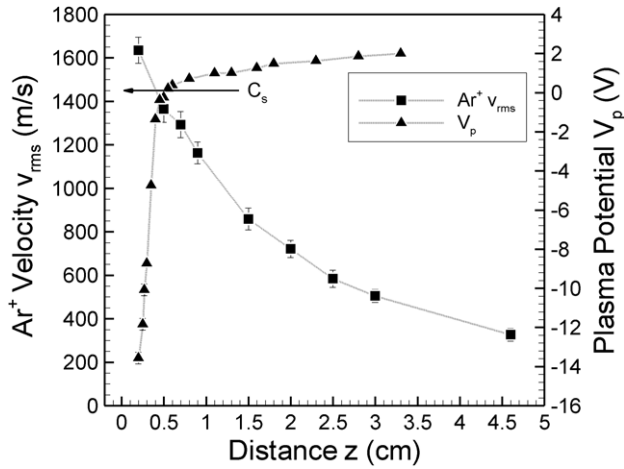
Figure 7. The spatial profile of the plasma potential (V_p) and argon ion velocity (v_{rms}) in the pure argon plasma. At the sheath edge ($z = 0.35$–0.40 cm), the rms velocity is the Bohm velocity (C_s) within the error range. It also agrees with the measured ion sound speed (v_{ph}) in the bulk.
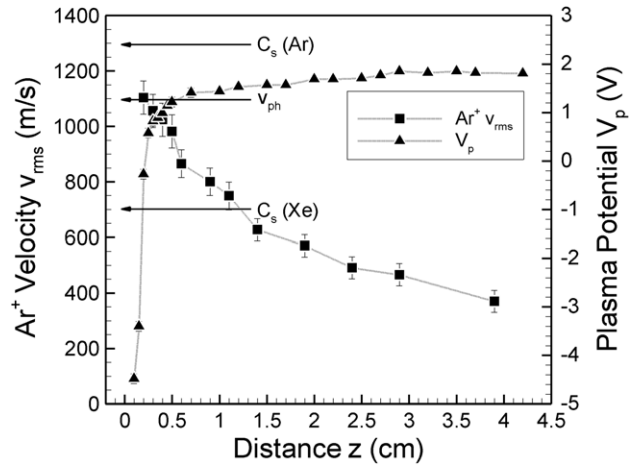

Figure 9. The spatial profile of the plasma potential (V_p) and argon ion velocity (v_{rms}) in the Ar 0.5 + Xe 0.2 mTorr plasma. At the sheath edge ($z = 0.25$–0.30 cm), the Ar^+ rms velocity is evidently slower than its own Bohm velocity and approaches the ion sound speed of the system (v_{ph}) in the bulk.

Figure 8. The spatial profile of the plasma potential (V_p) and argon ion velocity (v_{rms}) in the Ar 0.5 + Xe 0.1 mTorr plasma. At the sheath edge ($z = 0.25$–0.30 cm), the Ar^+ rms velocity is slower than its own Bohm velocity and approaches the ion sound speed of the system (v_{ph}) in the bulk.
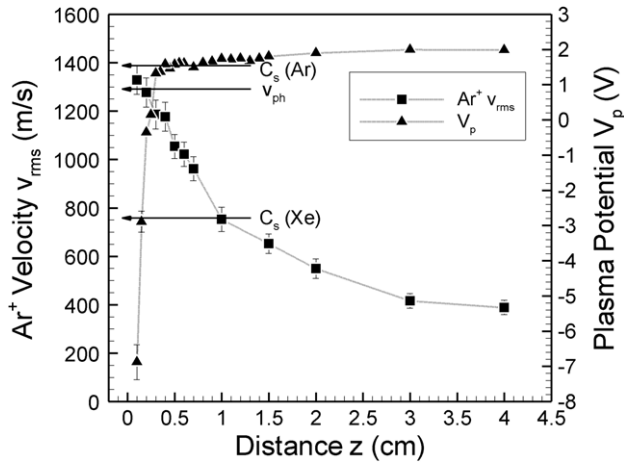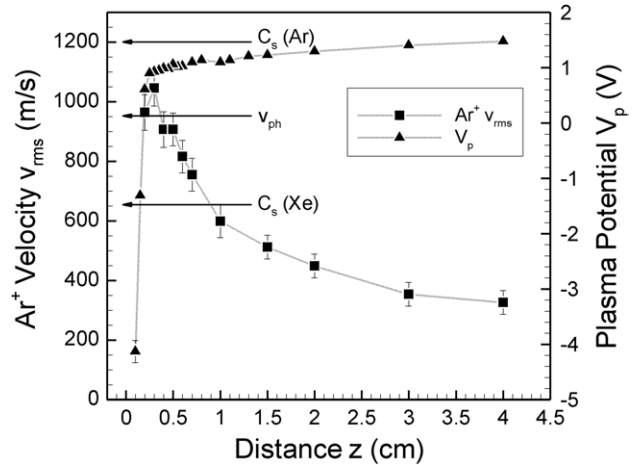

Figure 10. The spatial profile of the plasma potential (V_p) and argon ion velocity (v_{rms}) in the Ar 0.5 + Xe 0.3 mTorr plasma. At the sheath edge ($z = 0.15$–0.20 cm), the Ar^+ rms velocity is evidently slower than its own Bohm velocity and approaches the ion sound speed of the system (v_{ph}) in the bulk.

the magnetic fields used in our experiments (≈ 2.5 Gauss in the centre), other broadening effects such as Zeeman, power, natural, pressure and instrumental broadenings could be ignored. Using (6), the ion temperature of the ivdf in figure 6 is 0.032 ± 0.002 eV (≈ 102°C), consistent with the previous result [24].

Figure 7 shows the plasma potential profile and calculated argon ion velocity as a function of the distance z in the pure argon plasma. The argon neutral pressure is 0.7 mTorr and the electron density is 3.48×10^9 cm^{-3}. The effective electron temperature calculated from (4) is 0.88 eV which yields the Bohm velocity $C_s = 1460$ m s^{-1}. The emissive probe measurements give the plasma potential profile in the plasma. A presheath exists in a relatively long region and there is a sheath where the plasma potential decreases rapidly near the plate. Using the method to decide the sheath–presheath boundary explained above, the sheath edge is determined to

be $z = 0.35$–0.40 cm. The argon ion velocity at the sheath edge is 1450 ± 50 m s^{-1}, which matches fairly well with its Bohm velocity C_s. The measured IAW velocity v_{ph} is 1450 ± 10 m s^{-1}, so the three velocities coincide. The results verify that the argon ions reach their own Bohm velocity near the sheath edge which is same as v_{ph} in the bulk region, as expected by the Bohm criterion in single-species plasmas.

3.2. Argon ion velocities in argon–xenon plasmas

To generate a two-ion species plasma, neutral xenon is added to the argon plasma. Contrary to the previous Ar–He experiment where the argon was a heavier ion species [12, 13], the argon is now a lighter ion species. Figure 8 shows the plasma potential profile and calculated argon rms velocity as a function of the distance z in the argon–xenon plasma. The neutral argon pressure is 0.5 mTorr and 0.1 mTorr of xenon is mixed. The

Table 1. Summary of the results found from the Ar–Xe plasmas in figures 8, 9 and 10.

Figure	Sheath edge (cm)	n_e (cm^{-3})	T_e (eV)	C_{Ar} (m s^{-1})	C_{Xe} (m s^{-1})	IAW v_{ph} (m s^{-1})	n_{Ar}/n_e	n_{Xe}/n_e	v_{rms} (m s^{-1})
8	0.25–0.30	4.78×10^9	0.80	1390	770	1280 ± 10	0.78	0.22	1200 ± 60
9	0.25–0.30	5.71×10^9	0.68	1280	710	1090 ± 40	0.61	0.39	1080 ± 50
10	0.15–0.20	8.35×10^9	0.60	1200	660	960 ± 20	0.47	0.53	960 ± 50

electron density is 4.78×10^9 cm^{-3} and the effective electron temperature calculated from (4) is 0.80 eV which yields $C_{Ar} = 1390$ m s^{-1} and $C_{Xe} = 770$ m s^{-1} (arrows in figure 8). The IAW velocity v_{ph} is measured to be 1280 ± 10 m s^{-1}, so the relative ion concentrations from (5) are $n_{Ar}/n_e = 0.78$ and $n_{Xe}/n_e = 0.22$. The sheath edge is determined to be $z = 0.25$–0.30 cm by the emissive probe measurement. The argon velocity measured from the LIF data at the sheath edge is 1200 ± 60 m s^{-1} that is somewhat slower than v_{ph} but is between the Bohm velocities of the argon and xenon. The previous experiments in the Ar–He plasmas suggested that at the sheath edge the argon ions would reach the ion sound speed of the system which was the same as v_{ph} in the bulk region [12–14]. Our experiments confirm that the argon ions are slower than their own Bohm velocity (C_{Ar}) and approach the ion sound speed of the system (v_{ph}) at the sheath boundary when argon is the lighter ion species.

Different mixing ratios of argon and xenon are tried and the results are illustrated in figures 9 and 10. The argon pressure is fixed at 0.5 mTorr and added neutral xenon pressures are 0.2 mTorr and 0.3 mTorr in figures 9 and 10, respectively. The results are summarized in table 1. In the different mix ratios, the argon ions velocities are always slower than their own Bohm velocities, approaching the speed equal to the ion sound speed of the system. It is worth pointing out that except for the first mixture, the relative fraction of Xe II ions significantly exceeds the relative fraction of Xe I neutrals. In summary, our results combined with the previous ones indicate that the velocity of each ion species approaches the other near the sheath–presheath boundary and the common velocity is the ion sound speed of the system.

4. Conclusion

The generalized Bohm criterion has been studied experimentally in the cases of the pure Ar plasma and two-ion species Ar–Xe plasmas. The LIF findings showed that the argon ions approached their own Bohm velocity near the sheath boundary in the pure argon plasma. The previous IAW experiments combined with the LIF data in the Ar–He plasma where the argon was the heavier ion species suggested that both ions reached the ion sound speed of the system in the bulk near the sheath boundary. In our Ar–Xe plasmas where the argon was the lighter ion species, the argon ion velocity that it attained at the sheath edge was significantly slower than its own Bohm velocity and accelerated to the ion sound speed of the system. This predicted that the xenon ions also have the same speed as the argon ions near the sheath boundary in the Ar–Xe plasmas.

References

[1] Bohm D 1949 *The Characteristics of Electrical Discharges in Magnetic Field* ed A Guthrie and R K Wakerling (New York: McGraw-Hill) chapter 3
[2] Oksuz L and Hershkowitz N 2002 *Phys. Rev. Lett.* **89** 145001
[3] Oksuz L and Hershkowitz N 2005 *Plasma Sources Sci. Technol.* **14** 201
[4] Nakano T, Sadeghi N, Trevor D J, Gottscho R A and Boswell R W 1992 *J. Appl. Phys.* **72** 3384
[5] Kushner M J 1985 *J Appl. Phys.* **58** 4024
[6] Wenig G, Scheubert J and Awakowicz P 2003 *Surf. Coat. Technol.* **174–175** 482 (and references therein)
[7] Riemann K-U 1995 *IEEE Trans. Plasma Sci.* **23** 709
[8] Valentini H-B and Herrmann F 1996 *J. Phys. D: Appl. Phys.* **29** 1175
[9] Franklin R N 2000 *J. Phys. D: Appl. Phys.* **33** 3186
[10] Franklin R N 2001 *J. Phys. D: Appl. Phys.* **34** 1959
[11] Hala A M A 2000 Presheaths in Two Ion Species Plasma *PhD Dissertation* University of Wisconsin-Madison, College of Engineering
[12] Severn G D, Wang X, Ko E and Hershkowitz N 2003 *Phys. Rev. Lett.* **90** 145001
[13] Severn G D, Wang X, Ko E, Hershkowitz N, Turner M M and McWilliams R 2006 *Thin Solid Films* **506–507** 674
[14] Wang X and Hershkowitz N 2006 *Phys. Plasmas* **13** 053503
[15] Hoskinson A R and Hershkowitz N 2006 *Plasma Sources Sci. Technol.* **15** 85
[16] Severn G D, Edrich D A and McWilliams R 1998 *Rev. Sci. Instrum.* **69** 10
[17] Goeckner M J, Goree J and Sheridan T E 1991 *Phys. Fluids* B **3** 2913
[18] Keesee A M and Scime E E 2004 *Rev. Sci. Instrum.* **75** 4091
[19] Woo H-J, Chung K-S, Lho T and McWilliams R 2006 *J. Korean. Phys. Soc.* **48** 260
[20] Smith J R, Hershkowitz N and Coakley P 1979 *Rev. Sci. Instrum.* **50** 210
[21] Wang X and Hershkowitz N 2006 *Rev. Sci. Instrum.* **77** 043507
[22] Song S B, Chang C S and Choi D-I 1997 *Phys. Rev.* E **55** 1213
[23] Hala A M A and Hershkowitz N 2001 *Rev. Sci. Instrum.* **72** 2279
[24] Oksuz L, Atta Khedr M and Hershkowitz N 2001 *Phys. Plasmas* **8** 1729